ADOPD: A LARGE-SCALE DOCUMENT PAGE DECOMPOSITION DATASET

Jiuxiang Gu[1]* **Xiangxi Shi**[2] **Jason Kuen**[1] **Lu Qi**[3] **Ruiyi Zhang**[2] **Anqi Liu**[4]
Ani Nenkova[1] **Tong Sun**[1]
[1]Adobe Research [2]Oregon State University [3]UC, Merced [4]Johns Hopkins University

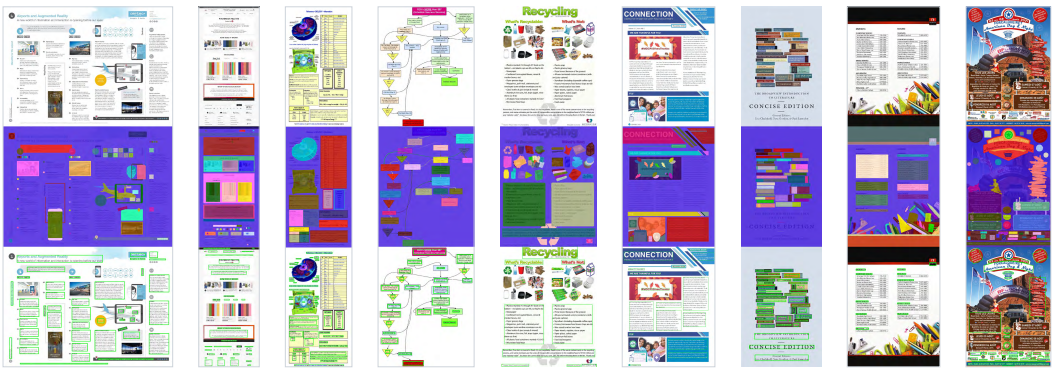

Figure 1: Overview of the ADOPD dataset showcasing densely annotated images of diverse document types and layouts. Each column displays the original image alongside Doc2Mask (colored masks) and Doc2Box (green boxes) annotations, organized from top to bottom.

ABSTRACT

Research in document image understanding is hindered by limited high-quality data. To address this, we introduce ADOPD, a comprehensive dataset for document page decomposition. ADOPD stands out with its innovative data-driven approach for document taxonomy discovery during data collection, complemented by dense annotations. Our approach integrates large-scale pretrained models with a human-in-the-loop process to guarantee diversity and balance in the resulting data collection. Leveraging our data-driven document taxonomy, we collected and densely annotated labels for document images, covering four document image understanding tasks: Doc2Mask, Doc2Box, Doc2Tag, and Doc2Seq. Specifically, for each image, the annotations include human-labeled entity masks, text bounding boxes, as well as automatically generated tags and captions that have been manually cleaned. We conduct comprehensive experimental analyses to validate our data and assess the four tasks using various models. We envision ADOPD as a foundational dataset with the potential to drive future research in document understanding[1].

1 INTRODUCTION

Document understanding research has been invigorated by the introduction of large-scale document datasets (Zhong et al., 2019; Mondal et al., 2020; Cheng et al., 2023) supporting a variety of document-related tasks (Mathew et al., 2021; Mathur et al., 2023). Yet document datasets still fall short compared to data resources in more established fields (Caron et al., 2021), in which advances have been so great that models and solutions can be incorporated in real-world applications. A case in point is the field of image decomposition, where progress was fueled by datasets like MSCOCO (Lin et al., 2014) and Pascal VOC (Everingham et al., 2010). Building a document page decomposition dataset of comparable quality is essential to advance document understanding research.

*Correspondence to: jigu@adobe.com

[1]For more information, please visit our project page: https://adopd2024.github.io

We construct ADOPD by addressing two important questions: *(1) How do we gather document data, and what types of documents should be included in the dataset?* Table 1 compares ADOPD with earlier datasets for document layout analysis (Mondal et al., 2020; Smock et al., 2022; Landeghem et al., 2023; Saad et al., 2016)[2]. Most datasets are sourced from PDFs, with limited document types. Models trained on such homogeneous data are unlikely to perform well on different types of documents, so a top prority when collecting ADOPD is to maximize the diversity of documents types in it. *(2) What elements should be annotated in document images for page decomposition?* Documents, with their varied forms, can be interpreted differently based on an individual's background. Document understanding encompasses intricacies such as visuals, text, and layout. For instance, a poster with a form may visually seem like a form, yet its text could classify it as a science or education book. The complex nature of document data poses challenges in hierarchically structuring it, a critical aspect for successful vision datasets like ImageNet and MSCOCO. Meanwhile, accurately describing the content of documents is highly valuable, but it is also more challenging than natural image captioning.

We explore the fundamental question: *How can we obtain a reasonable taxonomy of document types*? Pre-defining a fixed taxonomy solely based on human knowledge is not practical. Instead we assume an open taxonomy and make use of a data-driven taxonomy discovery method, gradually assembling the taxonomy through large-scale data exploration. Relying solely on manual annotation of document types, which requires reading and understanding the document content, is also not practical. Therefore, we leverage the powerful zero-shot capabilities of large pretrained models such as CLIP (Radford et al., 2021) and Large Language Models (LLM) (Floridi & Chiriatti, 2020) to assist in data selection and analysis. We couple the language model with methods for out-of-distribution (OOD) detection (Gu et al., 2023) for outlier data selection, complemented by a human-in-the-loop approach to achieve data diversity. Each ingredient in our proposed approach—LLM, OOD and human—is imperfect, but together they support the selection and annotation of diverse data at scale, within a reasonable budget.

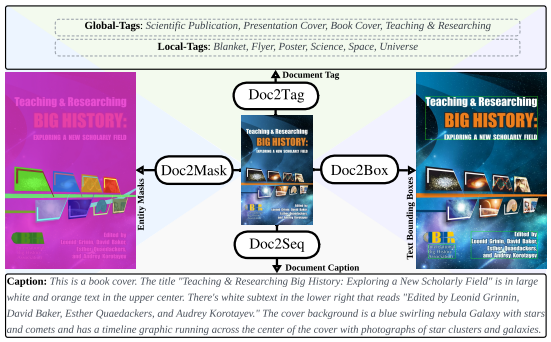

Figure 2: ADOPD page decomposition illustration.

Fig. 1 illustrates the diverse document types in ADOPD, comprising visually and textually rich documents, posing an annotation challenge despite its advantage. For visually rich documents like posters and diagrams, entity masks capture relationships between visual elements effectively. Conversely, for text-rich documents such as letters and articles, text bounding boxes are more suitable for marking key textual elements. To accomodate both types, we segment each document into entity masks and text box regions, and provide two types of descriptive labels for each document image. Fig. 2 showcases the four document page tasks: entity segmentation (Doc2Mask), text detection (Doc2Box), tagging (Doc2Tag), and captioning (Doc2Seq).

Table 1: Comparison of document datasets.

Dataset	Year	Size	Anno (Type)	Category
PubLayNet	2019	360K	Bbox (🖥)	📄 (1)
DocBank	2020	500K	Bbox (🖥)	📄 (1)
IIIT-AR-13K	2020	13k	Bbox (👥)	🖼 (1)
DocLayNet	2022	80.9k	Bbox (👥)	📄 (6)
M^{6}Doc	2023	9.1k	Bbox (👥)	📄🖼 (7)
ADOPD (**Ours**)	2023	120k	Polygon (👥) Text Bbox (👥) Caption (🤖) Tag (🤖+ 👥)	🖼 (>1000)

In sum, ADOPD is a large-scale diverse document page decomposition and description dataset, designed to support future research in document domain. In this paper, we:

- present ADOPD, comprehensive dataset for document page decomposition, encompassing four distinct tasks: Doc2Mask, Doc2Box, Doc2Seq, and Doc2Tag.
- propose a data-driven approach for constructing document taxonomies during data collection and safeguard the ADOPD through outlier detection and human-in-the-loop.
- conduct extensive experiments and analysis on ADOPD, demonstrating its effectiveness and generalization capabilities for document understanding research.

[2]The symbol 🖥 indicates automatic annotations, 👥 represents human annotations, and 🤖 signifies LLM assistance. 📄 indicates that the document source is a digital PDF, while 🖼 indicates document images.

2 RELATED WORK

Document Datasets. As shown in Table 1, several recent document image datasets have been introduced. PubLayNet (Zhong et al., 2019) comprises images and annotations generated through the automated alignment of PDFs with XML formats. DocBank (Li et al., 2020b) is created using LaTeX-generated PDF files and employs an efficient weakly supervised approach for annotation. DocLayNet (Pfitzmann et al., 2022) relies on human annotation rather than automated methods. This dataset encompasses six distinct document types and encompasses a total of 11 annotation categories. M^6Doc (Cheng et al., 2023) is a recently introduced dataset featuring approximately 9k modern document images, divided into seven subsets. It contains detailed annotations spanning multiple distinct categories. IIIT-AR-13K (Mondal et al., 2020) is tailored for object detection in business documents like annual reports, containing annotated pages with standard layout elements like text, headings, lists, graphics, and tables. In summary, existing large-scale document image datasets mainly focus on PDFs, unlike the varied scanned or photographed images encountered in real-world scenarios. This limited distribution of data can bias trained models. Additionally, publicly available datasets often cover only a narrow range of document layouts and categories.

Document Models. The document domain has witnessed the emergence of foundational models (Li et al., 2020a; Prasad et al., 2020), *etc*. fueled by advancements in deep learning. Despite the rapid development of document understanding models, the scarcity of high-quality large-scale document data remains a significant challenge. Earlier document layout analysis methods (Ouwayed & Belaïd, 2012; Lee et al., 2019) relied heavily on rule-based and heuristic algorithms. However, their applicability was limited to simple document types, resulting in poor generalization performance. In addition to task-driven models, researchers have proposed a range of document pretraining models (Huang et al., 2022; Li et al., 2021; Gu et al., 2021; Tang et al., 2023; Kim et al., 2022). These models are typically pretrained on the IIT-CDIP (Lewis et al., 2006) dataset and evaluated on various document benchmarks. Despite the remarkable performance of these models on benchmark datasets, it is critical to acknowledge that most current image-based document datasets are predominantly composed of a narrow range of document types, failing to capture the heterogeneity of real-world documents. Moreover, the restricted data diversity in these benchmark datasets constrains the development and evaluation of document models.

3 ADOPD DATASET

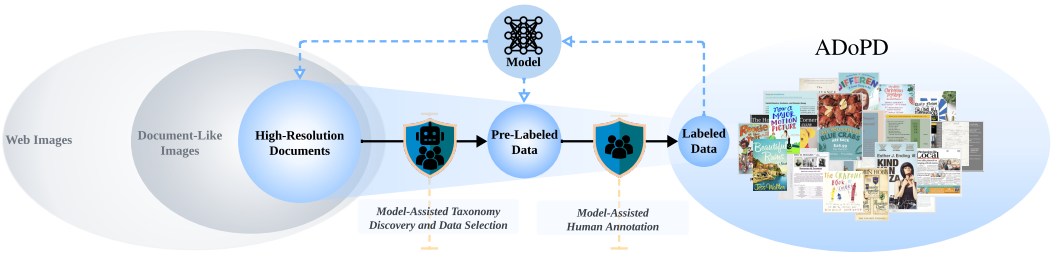

Figure 3: Model-assisted data collection and annotation pipeline for ADOPD.

ADOPD stands out among document datasets as it is constructed using diverse document images found on the web. Sec. 3.1 introduces document page decomposition tasks, while Sec. 3.2 presents a data-driven approach to discovering document taxonomy for data collection and analysis. Sec. 3.3 employs models to assist with human annotation, addressing challenges posed by diverse data.

3.1 TASK DEFINITION

Fig. 2 illustrates the document page decomposition task defined in this paper, which encompasses four subtasks: Doc2Mask, Doc2Box, Doc2Seq, and Doc2Tag.

- The Doc2Mask task entails segmenting visual entities in document images in a class-agnostic manner. An “entity" in this context denotes a thing (instance) mask or a stuff mask. For example, in Fig. 1, an entity represents a meaningful and coherent region (*e.g*., banner, figure, logo, *etc*).
- The Doc2Box task calls for identifying text region-of-Interest (RoI) within a document image, regardless of their specific types. The term “box" refers to text RoI (*e.g*., paragraphs and titles, *etc*).

- The Doc2Seq task involves generating captions for document images, requiring the model to analyze visual elements and structured text. Given the complexity of document images, the model must effectively comprehend visual, textual, and layout information to produce detailed captions.
- The Doc2Tag task is akin to image tagging, specifically multi-label image recognition, where the objective is to assign multiple semantic labels to an image. In Doc2Tag, two levels of tagging are utilized: one based on the overall image content and another on specific local regions.

3.2 DATA-DRIVEN DOCUMENT TAXONOMY DISCOVERY

In standard classification scenario, we deal with a given dataset denoted as $\mathcal{D}_{\text{full}}$, where $\mathcal{X}$ represents the input space, and $\mathcal{Y} = \{1, \ldots, K\}$ is the label space. The classification model, denoted as $f := g \circ h$, consists of a feature extractor $h : \mathcal{X} \to \mathbb{R}^d$ and a classifier $g : \mathbb{R}^d \to \mathbb{R}^K$, which maps the input's feature embedding to K real-valued numbers called logits. In practice, establishing a guiding taxonomy associated with K is crucial for effective data collection, enabling us to manage and assess the diversity of the collected data. However, determining an appropriate value for K in documents is challenging due to the diversity of documents. We draw inspiration from pretrained models such as CLIP, GPT-4, *etc*, which have been trained on large-scale datasets and can serve as knowledgeable "experts" for data selection. Despite the benefits of pretrained models, the predictions from such models are not always reliable. *E.g.*, LLMs[3] tend to suffer from hallucination problems (Bang et al., 2023). Hence, incorporating safeguards into data collection is essential. Fig. 3 provides an overview of our data collection process, which will be detailed in the subsequent sections.

Can Large-Scale pretrained Models Facilitate Data Collection? Given a document image $x \sim \mathcal{D}_{\text{full}}$, we can extract document information using pre-existing models as follows:

$$\{\boldsymbol{z},\ S_{\text{OCR}},\ S_{\text{Caption}},\ S_{\text{Attribute}},\ S_{\text{Label}}\} = \{h(x),\ f_{\text{OCR}}(x),\ f_{\text{I2T}}(x),\ f_{\text{Tag}}(x),\ f_{\text{CLIP}}(x|\mathcal{Y})\} \quad (1)$$

$$\{S^*_{\text{Caption}},\ S^*_{\text{Tag}}\} = \text{LLM}(\ S_{\text{OCR}},\ S_{\text{Caption}},\ S_{\text{Attribute}},\ S_{\text{Label}}|\text{Prompt}) \quad (2)$$

where $\boldsymbol{z} \in \mathbb{R}^D$ is obtained through an image feature extractor $h(\cdot)$. The sequence S_{OCR} consists of words and their coordinates, extracted by OCR tool $f_{\text{OCR}}(\cdot)$. The caption S_{Caption} is generated by the captioning model $f_{\text{I2T}}(\cdot)$. Tags $S_{\text{Attribute}}$ are produced by the image tagging model $f_{\text{Tag}}(\cdot)$. Labels S_{Label} are generated by the CLIP model $f_{\text{CLIP}}(\cdot|\mathcal{Y})$, constrained by $\mathcal{Y}$. Integrating multimodal information, as expressed in Eq.1, for document reasoning poses a significant challenge. As demonstrated in Eq.2, we harness the power of LLMs and formulate prompts to predict tags (S^*_{Tag}) and captions (S^*_{Caption}) for document images. The ablation study of these prompts is explored in the Appendix.

How to Safeguard Data Collection? Despite the impressive zero-shot capabilities of LLMs for sequence reasoning, prediction errors and uncertainties may still arise. Some failure cases can be addressed with stricter prompts. Even so, fully relying on LLMs for data selection poses heavy risks.

Fig. 4 illustrates our data selection diagram, strengthened by outlier detection. For each batch of sampled web images ($\mathcal{D}_{\text{selected}}$), we define it as a mix of in-distribution (ID) ($\mathcal{D}_{\text{pseudo-in}}$) and OOD ($\mathcal{D}_{\text{pseudo-out}}$) data. In $\mathcal{D}_{\text{pseudo-in}}$, all samples belong to taxonomy classes we have already explored, while $\mathcal{D}_{\text{pseudo-out}}$ comprises samples from document types we haven't explored yet. Alg. 1 outlines the process where we integrate outlier detection for data collection and taxonomy discovery. Given the dataset pool denoted as $\mathcal{D}^t_{\text{full}}$ and t indicates the time step, we initially select a batch of data, denote as $\mathcal{D}^t_{\text{selected-in}}$, from $\mathcal{D}_{\text{full}}$. Based on the current taxonomy $\mathcal{Y}^t$, we first partition $\mathcal{Y}^t$ into 100 clusters using the K-means algorithm (Jiang et al., 2024). Afterwards, we sample $\mathcal{D}^t_{\text{pseudo-in}}$ from $\mathcal{D}^t_{\text{selected-in}}$ based on the K clusters, corresponding to step ① in Fig. 4. Specifically, we randomly select a sub-category y^t_k from cluster k as the representative category. We then use CLIP to sample n^t documents classified under y^t_k. The pseudo input ID data $\mathcal{D}^t_{\text{pseudo-in}}$ comprises a total of $100 \cdot n^t$ document images. This selection process ensures a balanced sampling operation within the current taxonomy $\mathcal{Y}^t$.

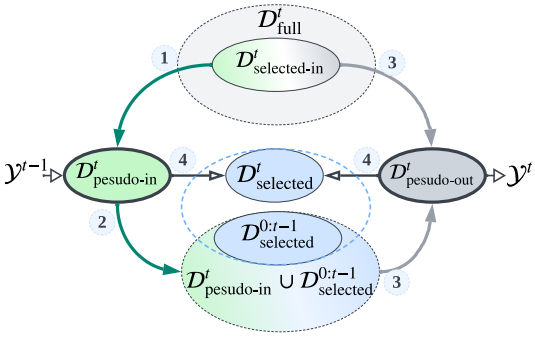

Figure 4: Data selection diagram for ADOPD.

[3]Without specific indication, LLM in this paper refers to GPT-4.

Sampling from ID data can lead to biased distributions because models trained on such data may silently fail when faced with OOD inputs. Therefore, enhancing the diversity of ADOPD by incorporating hard negative examples may result in an overall improvement in diversity. Therefore, we explicitly sample a OOD subset $\mathcal{D}^t_{\text{pseudo-out}}$ from the current candidate pool $\mathcal{D}^t_{\text{selected-in}} \setminus \mathcal{D}^t_{\text{pseudo-in}}$, corresponding to step ③ in Fig. 4. To obtain $\mathcal{D}^t_{\text{pseudo-out}}$, we employ K-means to segregate outliers from $\mathcal{D}^t_{\text{selected-in}}$. Specifically, we extract image features $\bar{\mathbf{Z}}^t$ for $\mathcal{D}^{0:t-1}_{\text{selected}} \cup \mathcal{D}^t_{\text{selectd-in}}$, where $\mathcal{D}^{0:t-1}_{\text{selected}} = \mathcal{D}^{0:t-1}_{\text{pseudo-in}} \cup \mathcal{D}^{0:t-1}_{\text{pseudo-out}}$. In this context, $\bar{\mathbf{Z}}^t = \bar{\boldsymbol{z}}^t_k$, with $k \in [0, 100)$ representing the set of K-means centroids estimated from $\mathcal{D}^{0:t-1}_{\text{selected}} \cup \mathcal{D}^t_{\text{pseudo-in}}$. The outlier score is estimated as the Euclidean distance between it and the nearest centroid:

$$s^t(\boldsymbol{z}) = \min_{k \in [0,100)} ||\boldsymbol{z} - \bar{\boldsymbol{z}}^t_k||_2, \quad \boldsymbol{z} \in (\mathcal{D}^t_{\text{selected-in}} \setminus \mathcal{D}^t_{\text{pesudo-in}}) \tag{3}$$

where $\mathcal{D}^t_{\text{pseudo-out}}$ contains data points with outlier scores ranked in the top n^t across K clusters.

Given the selected ID and OOD data, we have $\mathcal{D}^t_{\text{selected}} = \mathcal{D}^t_{\text{pseudo-in}} \cup \mathcal{D}^t_{\text{pseudo-out}}$, which is ready for annotation (step ④ in Fig. 4). Before annotation, we update $\mathcal{Y}^{t-1}$ by using the newly selected data $\mathcal{D}^t_{\text{selected}}$. Here, we employ the approach outlined in Eq. 2, leveraging the LLM to predict the presence of new labels and obtain the updated taxonomy $\mathcal{Y}^t$. We use prompt-based methods to predict document tags by considering four aspects: *visual* ($\mathscr{P}_{\text{visual}}$), *textual* ($\mathscr{P}_{\text{textual}}$), *layout* ($\mathscr{P}_{\text{layout}}$), and *multimodal* ($\mathscr{P}_{\text{multimodal}}$). Each aspect is addressed through unique input combinations in the prompt. Additional details about the prompts can be found in the Appendix. After obtaining outputs, we implement two safeguards to filter out failures. Firstly, we design a prompt-based summarizer ($\mathscr{P}_{\text{summary}}$) using LLM to obtain 10 tags by summarizing the tags predicted through the four prompt strategies. Secondly, after the label generation by LLM, human annotators review and eliminate labels that are confusing or irrelevant to the document.

Algorithm 1: Data-Driven Taxonomy Discovery

Input : $\mathcal{Y}^0$, $\mathcal{D}_{\text{full}}$, ϵ.
Output: Expanded Taxonomy $\mathcal{Y}$
while *True* **do**
  ① Collect $\mathcal{D}^t_{\text{select-in}}$ from $\mathcal{D}^t_{\text{full}}$;
  ② Select $\mathcal{D}^t_{\text{pseudo-in}}$ from $\mathcal{D}^t_{\text{selected-in}}$ based on $\mathcal{Y}^{t-1}$;
  ③ Generate image embeddings $\mathbf{Z}$ for $\mathcal{D}^{0:t-1}_{\text{selected}} \cup \mathcal{D}^t_{\text{pesudo-in}}$;
  ③ Calculate $s^t(\boldsymbol{z}), \forall \boldsymbol{z} \in (\mathcal{D}^t_{\text{selected-in}} \setminus \mathcal{D}^t_{\text{pesudo-in}})$;
  ③ Select outlier data $\mathcal{D}^t_{\text{pesudo-out}}$;
  foreach $x \sim \mathcal{D}^t_{\textit{pesudo-in}} \cup \mathcal{D}^t_{\textit{pesudo-out}}$ **do**
    ④ Predict new labels using four prompters;
    ④ Update $\mathcal{Y}^t$ with the newly predicted labels;
  ④ Refine $\mathcal{Y}^t$ with human annotator;
  if $|\mathcal{Y}^t| > \epsilon$ **then**
    Stop;
  else
    $t \leftarrow t + 1$;

3.3 Model-Assisted Data Annotation

Data Collection. The images in ADOPD are sourced from the Laion-HR (Laion High Resolution), which comprises high-resolution web images, including multilingual document images. Laion-HR provides a foundation for our multi-lingual multi-modal ADOPD. We leverage pretrained models with humans in the loop to collect and filter data. The process includes the following steps:

- *Model-Assisted Data Selection*: We first select images based on Laion-HR's metadata by applying criteria such as pwatermark < 0.8 and punsafe < 0.5. Then, we construct a document discovery dataset using natural image datasets (*e.g.*, ImageNet, *etc*) and document datasets (*e.g.*, DocLayNet, *etc*). We then finetune a DiT-based binary image classifier (Li et al., 2022a) to identify potential documents (probability > 0.8). Subsequently, we apply an OCR tool (Du et al., 2021), and retain those with a word count exceeding 10. Although metadata provides predictions for watermarks, in order to improve accuracy, we additionally train a watermark detection model to filter watermarked images. We compute MD5 hashes and Hamming distances between images to exclude duplicates, even if document images in Laion-HR have different URLs. Fig. 10 in the Appendix shows the percentage of data selection.
- *Human Selection and Sensitive Verification*: Based on our taxonomy[4] obtained by Alg. 1, we adopt pretrained CLIP model for zero-shot tagging. Human annotators then select safe and valid images for all categories. We do not rigidly specify that images must be print-format documents, but instead suggested the annotators to choose those that resemble documents. Annotators are tasked with filtering the dataset for potentially sensitive information.

[4]Note that the taxonomy $\mathcal{Y}$ gradually change with the growth of data collection.

Data Annotation. The annotation process of ADOPD prioritizes the core principle of *understanding the document's structure and layout*. We avoid imposing overly rigid constraints on annotation.

- *Model-Assisted Manual Annotation*: In the early stage, we utilize a pretrained CropFormer (Qi et al., 2023) to generate pseudo entity masks. Annotators follow guidelines to adjust the masks by adding, modifying, or deleting as needed. After annotating a sufficient amount of data, CropFormer is retrained with the new annotations and serves as the seed model for data preprocessing in the subsequent stage. Through this iterative process, our model progressively reduces annotation costs while simultaneously increasing annotation efficiency. Fig. 12 in the Appendix illustrates the effectiveness of model-assisted annotation. During the annotation process, we provide document captions (S^*_{Caption}) and tags (S^*_{Tag}) to aid annotators in understanding the document.
- *Multi-Task and Multi-Lingual Annotation*: ADOPD stands out from other document datasets for its multi-task and multi-lingual characteristics. Our primary focus is on English and CJK (Chinese, Japanese, Korean) documents, with 60k document images in English and the remaining in the other languages. We reserve a private test set for the competition. Each dataset has four tasks introduced in Sec. 3.1. Specifically, for Doc2Mask annotation, we refrain from imposing semantic constraints on labeling entities, therefore encouraging annotators to come up with open-ended names or descriptions that are accurate (*e.g.*, "*doc-in-doc*", "*banner*", "*infographic*", "*natural image*", *etc*). As our task focuses on document entity segmentation, we do not incorporate label information in segmentation evaluations. For Doc2Box, we have stricter rules which require annotators to comprehend words and group them according to their semantic meaning. The annotation files follow the MSCOCO annotation format. The comprehensive guidelines, along with the complete dataset, will be available for reference.

4 EXPERIMENTS

4.1 IMPLEMENTATION DETAILS

Baseline Models. We experiment on the subset of ADOPD, with training and validation sets comprising 50k and 10k images, respectively. **(1)** Doc2Mask: we evaluate two frameworks: Mask2Former (Cheng et al., 2021) and CropFormer (Qi et al., 2023), to identify which is best stuited for the document page decomposition task. We perform ablation studies on these frameworks using different backbones, such as Swin Transformer (Swin) (Liu et al., 2021), Hornet (Rao et al., 2022), and ViT (Parmar et al., 2018). **(2)** Doc2Box: we similarly benchmark three models: Faster R-CNN (Ren et al., 2015), Deformable-DETR (Zhu et al., 2021), and Cascade Mask-RCNN (MR-CNN) (Cai & Vasconcelos, 2019). We also enhance Cascade Mask-RCNN by incorporating pretrained ViT backbones, specifically DINOv1 (Caron et al., 2021) and Dinov2 (Oquab et al., 2023) with ViT-Adapter (Chen et al., 2022). **(3)** Doc2Seq: we build an encoder-decoder model using pretrained ViT and GPT-2 (Radford et al., 2019), fine-tuned on 80k image-caption pairs for training and 20k for validation. The captions are generated using prompts specified in Eq. 2. Acknowledging the gap between LLM-generated and human annotations, we collect an extra 5k human-annotated validation set for further comparison. **(4)** Doc2Tag: we validate our taxonomy discovery using the CLIP ViT-G/14 model and report the OOD performance on RVL-CDIP (Harley et al., 2015).

We build Doc2Mask using the Detectron2 (Wu et al., 2019) and Doc2Box with MMDetection (Chen et al., 2019). All experiments are run on NVIDIA A100-80GB GPUs. Following standard practices(Ghiasi et al., 2021), we employ an input resolution of 1024×1024, achieved by re-scaling and padding the shorter side of the image. Doc2Mask (CropFormer and Mask2Former) and Doc2Box (Faster R-CNN, Cascade Mask-RCNN) are trained for 15 epochs with a batch size of 32 on 8 GPUs to achieve full convergence. We train Deformable-DETR for 30 epochs due to slow convergence issues. We build other models (Doc2Seq and Doc2Tag) with Huggingface Transformers framework (Wolf et al., 2020). For Doc2Seq, we train it for 50 epochs on 8 GPUs with a total batch size of 800. Finetuning CLIP ViT-G/14 on Doc2Seq data takes 100 epochs on 8x8 GPUs.

Evaluation Metrics. We evaluate Doc2Mask and Doc2Box with the mean average recall (mAR) and mean average precision (mAP) metrics. This assessment considers ten overlap thresholds ranging from 0.5 to 0.95 in increments of 0.05 (mAP@0.5-0.95). For OOD evaluation, we use metrics including the Area Under the Receiver Operating Characteristic (AUROC), False Positive Rate at 95% Recall (FPR95), maximum concept matching (MCM) score (Ming et al., 2022), and accuracy

(ACC). For Doc2Seq, we use the BLEU@n (B@n) (Papineni et al., 2002), CIDEr (C) (Vedantam et al., 2015), METEOR (M) (Denkowski & Lavie, 2014) and ROUGE (R) (Lin, 2004) for evaluation.

4.2 Document Page Decomposition Tasks Analysis

Comparing the Model Architectures. Table 2 compares Mask2Former and CropFormer models on Doc2Mask. CropFormer outperforms Mask2Former with similar backbones and pretrained datasets. CropFormer's superiority stems from its integration of image crops alongside full image input, enhancing mask prediction with detailed information. This highlights the model's ability to handle multi-view and local image information, especially in the context of document images.

We compare various object detection models in Table 3, including Faster R-CNN, Deformable-DETR, and Cascade MR-CNN. While Deformable-DETR improves, it doesn't outperform anchor-based detectors like Faster R-CNN and Cascade MR-CNN significantly. Despite achieving a higher mAR, the limited mAP improvement may be due to the distinct data distribution of text boxes, differing from general objects in natural images with clear classification boundaries. Meanwhile, the Cascade MR-CNN, combining Mask R-CNN and Cascade R-CNN, achieves the highest mAP. It enhances instance segmentation performance and aids text detection, especially for words requiring pixel-level feature representation.

Table 2: Results on Doc2Mask with varied backbones (T, B, L) denoting tiny, base, and large types.

	Backbone	Pretrain	Mask Quality			
			mAP	AP_{50}	AP_{75}	mAR
Mask2Former	$Swin_T$	EntitySeg	31.80	37.16	32.33	34.0
		ImageNet	28.95	34.36	29.51	31.0
	$Swin_L$	EntitySeg	32.81	38.14	33.17	35.3
		ImageNet	30.21	36.30	31.18	32.5
	$Hornet_L$	EntitySeg	34.39	40.09	34.95	36.9
		ImageNet	32.96	38.22	33.30	35.2
	ViT_B	SA-1B	35.59	41.05	36.35	37.6
	ViT_L		35.81	40.27	36.53	37.8
Cropformer	$Swin_T$	EntitySeg	35.46	41.56	35.60	38.5
		ImageNet	37.71	45.30	38.20	41.0
	$Swin_L$	EntitySeg	36.03	42.30	36.23	39.3
		ImageNet	37.73	44.62	38.49	40.7
	$Hornet_L$	EntitySeg	35.03	40.00	35.73	37.6
		ImageNet	36.06	41.84	36.69	38.7
	ViT_B	SA-1B	35.87	41.92	36.73	38.4
	ViT_L		39.56	45.72	40.33	42.4

Comparing Backbones and Pretraining. Table 2 also investigates the impact of vision backbone pretrained on various datasets. References to EntitySeg, ImageNet, and SA-1B indicate pretraining on the respective datasets. SAM (Kirillov et al., 2023) pretrained on SA-1B outperforms the Swin/Hornet models trained on ImageNet or EntitySeg. This can be attributed to two factors: firstly, SA-1B is sufficiently large (around 1 Billion). Secondly, while Swin/Hornet architectures are well-suited for segmentation, SAM is trained with pixel-level supervised learning, enabling it to acquire improved pixel-level representations crucial for document image understanding.

Table 3 compares different backbones on Doc2Box. $Dinov2_{P14}$ + $ViT_{Adapter}$ excels with higher mAP yet slightly lower mAR, demonstrating the superiority of self-supervised backbones over pretrained alternatives. This is crucial for document analysis, given the absence of high-quality ImageNet-like pretraining data. Comparing $Dinov1_{P8}$ and $Dinov1_{P16}$ suggests that fine-grained patches enhance document image features. Fig. 5b illustrates the results of Doc2Box using $Dinov2_{P14}$+$ViT_{Adapter}$.

Table 3: Performance comparisons on Doc2Box.

Method	Backbone	Box Quality			
		mAP	AP_{50}	AP_{75}	mAR
Faster R-CNN	$ResNet_{50}$	61.1	78.9	67.0	74.9
	$ResNet_{101}$	61.4	78.6	67.3	74.3
Deformable-DETR	$ResNet_{50}$	65.0	82.2	72.1	81.6
	$ResNet_{101}$	65.5	82.8	72.7	81.6
Cascade MR-CNN	$ResNet_{50}$	64.7	80.9	71.0	79.4
	$ResNet_{101}$	65.3	71.7	68.7	79.1
	$Dinov1_{P8}$+ $ViT_{Adapter}$	63.6	80.4	69.6	76.3
	$Dinov1_{P16}$+ $ViT_{Adapter}$	63.2	80.3	69.5	76.2
	$Dinov2_{P14}$+ $ViT_{Adapter}$	67.0	82.7	73.2	77.8

Evaluating Generalization Ability. In Table 4 (a), we compare the model trained on ADOPD with those fine-tuned on EntitySeg. Combined with Fig. 5a, it is evident that models fine-tuned on ADOPD can better focus on fine-grained document elements and make more reasonable predictions for document entity masks. Conversely, models pretrained on EntitySeg can predict some masks but tend to excessively detect elements present in natural images (*e.g.*, people, objects), while neglecting the document's inherent layout. Table 4 (b) validates the cross-dataset generalization pretraining advantage of ADOPD, specifically focusing on the evaluation set of DocLayNet. For a fair comparison, we consider only text detection without categorizing the boxes. Directly applying the model fine-tuned on ADOPD to DocLayNet data yields zero-shot results with high recalls. Furthermore, fine-tuning on DocLayNet with ADOPD pretrained backbones outperforms fine-tuning with ImageNet backbones. Note that DocLayNet's testing is limited to its limited document types and cannot reveal anything about the generalization capability of ADOPD for other taxonomy types.

Table 4: Ablation studies: (a) comparing the performance of models trained with ADOPD and models fine-tuned only on EntitySeg. The results in "(·)" represent the zero-shot outcomes for EntitySeg. (b) Cross-dataset evaluation to assess the generalizability of ADOPD on DocLayNet.

(a) Results for with and without ADOPD.

Backbone	mAP	AP_{50}	AP_{75}	mAR
Mask2Former				
$Swin_L$	32.81(16.27)	38.14(22.52)	33.17(15.88)	35.3(29.3)
$Hornet_L$	34.39(15.83)	40.09(21.74)	34.95(15.38)	36.9(29.0)
Cropformer				
$Swin_L$	36.03(13.46)	42.30(19.41)	36.23(13.12)	39.3(24.5)
$Hornet_L$	35.03(15.68)	40.00(21.39)	35.73(15.26)	37.6(26.9)

(b) Cross-dataset evaluation on DocLayNet.

Method	Backbone	Zero-Shot		Finetune			
		ADOPD		ImageNet		ADOPD	
		mAP	mAR	mAP	mAR	mAP	mAR
Faster R-CNN	$ResNet_{50}$	0.9	58.5	43.0	55.8	44.5	60.4
	$ResNet_{101}$	1.0	56.6	46.0	58.5	47.0	60.7
Deformable-DETR	$ResNet_{50}$	2.2	80.4	74.7	87.2	75.4	88.9
	$ResNet_{101}$	2.6	79.0	75.4	85.9	77.2	88.1

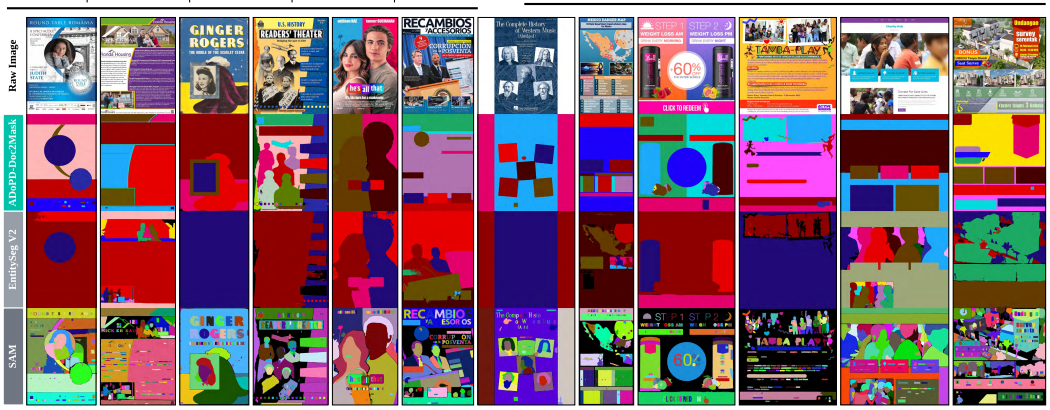

(a) Mask Prediction Comparison: From top to bottom, we showcase the original image and predictions from the best models trained on ADOPD, EntityV2, and SAM (SA1B), respectively.

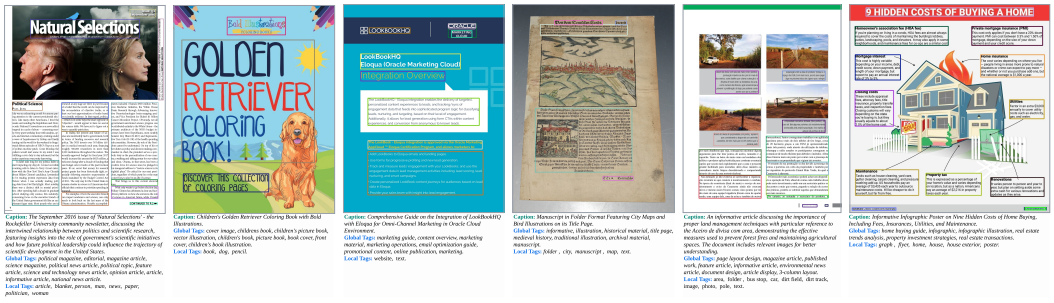

(b) Document text detection visualization results, each image paired with its caption and tags.

Figure 5: Visualization of ADOPD images and results for Doc2Mask and Doc2Box.

Prompt-Guided Context-Aware Captioning Benefits Vision-Language Modeling. Table 4.2 evaluates caption quality. We collect 5K test data to evaluate the effectiveness of Doc2Seq. The 🤖 represents the GPT-4 model, and $BLIP_{Large}$ (Li et al., 2022b) and BLIP2-OPT-2.7b (Li et al., 2023) are obtained from Huggingface model hub. ViTBase-P32-384/$ViT_{Base\text{-}P16\text{-}384}$+GPT2 are fine-tuned on Doc2Seq. While GPT-4 captions achieve a commendable CIDEr score, indicating consensus, a noticeable disparity persists between them and human annotations. Models fine-tuned on Doc2Seq can attain similar performance to GPT-4 on B@n, but show significantly lower CIDEr scores. In Fig. 6 (left), human-written captions are notably longer than machine-generated ones, impacting reference-based evaluation. These findings highlight the challenge in document captioning due to diverse interpretations and varying caption lengths, complicating evaluation.

To verify the benefits of prompt-guided captions, we fine-tune CLIP with Doc2Seq data and conduct two experiments: zero-shot evaluation on RVL-CDIP test set and supervised training on RVL-CDIP based on finetuned CLIP vision backbone. While finetuned CLIP improves zero-shot capability for specific data (*e.g.*, Budget and Presentation), the overall enhancement is comparable to raw pretrained CLIP. We observe from Fig. 6 (right) and Table 6 that finetuning the CLIP ViT backbone, initially trained on Doc2Seq, with a classifier layer for separate training on RVL-CDIP results in a noticeable improvement. This underscores the importance of caption rewriting for handling noisy data.

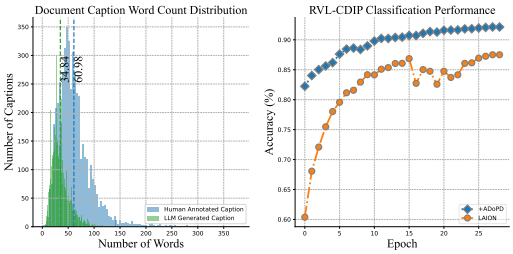

Figure 6: Ablation study on captions.

Method	Test	B@1	B@2	B@3	B@4	M	R	C
		27.0	16.7	11.7	8.5	12.8	22.4	84.7
$BLIP_{Large}$		12.4	8.5	6.4	5.0	9.3	22.6	18.3
		8.2	5.6	4.0	3.0	8.6	21.6	3.4
BLIP2-OPT-2.7b		4.3	3.6	3.0	2.6	10.7	25.1	16.5
		12.3	7.6	5.3	3.9	9.0	21.8	18.0
$ViT_{Base\text{-}P32\text{-}384}$+GPT2		22.5	9.2	4.4	2.5	7.7	16.8	9.8
		16.7	5.8	2.3	1.0	5.8	13.9	4.4
$ViT_{Base\text{-}P16\text{-}384}$+GPT2		23.4	9.7	4.7	2.7	8.0	17.2	11.0
		17.3	6.0	2.4	1.1	6.0	14.1	5.3

Table 5: Ablation experiments on Doc2Seq.

Table 6: Performance of Models for Per-Class Classification

Model	Type	Letter	Form	Email	Hw	Ad	SR	SP	SP	FF	NA	Bgt	Inv	Prsnt	Qnr	Rsm	Memo	Avg
Per-Class (Recall@5)																		
DiT_{base}	Supervised	98.92	98.76	99.45	98.99	99.64	97.86	99.84	99.31	99.52	99.18	99.24	98.83	99.76	99.15	99.28	99.16	99.18
$ViT_{G\text{-}14}$	Zero-Shot	98.52	98.76	79.78	91.89	53.46	76.51	87.64	84.82	32.81	99.49	33.07	99.35	54.81	93.75	90.46	98.23	79.58
$ViT_{G\text{-}14}$+ADOPD	Zero-Shot	94.32	87.55	75.33	85.79	27.46	80.33	96.21	63.46	38.72	98.79	65.81	93.93	72.26	84.25	84.41	95.02	77.73
Per-Class (Accuracy)																		
DiT_{base}	Supervised	92.41	86.83	98.97	96.13	94.63	87.11	95.22	94.90	96.68	92.77	92.73	94.07	87.38	90.84	97.67	95.14	93.36
$ViT_{G\text{-}14}$	Supervised	86.20	76.70	94.28	93.48	91.81	71.94	91.10	89.72	94.97	83.68	81.24	87.44	78.26	84.97	92.94	85.87	86.57
$ViT_{G\text{-}14}$+ADOPD	Supervised	90.87	84.48	96.98	95.34	93.76	82.39	93.51	93.00	95.61	89.81	89.62	92.85	84.29	90.23	96.45	92.62	91.38

[1] The abbreviations are: Handwritten (Hw), Advertisement (Ad), Scientific Report (SR), Scientific Publication (SP), Specification (Spec), File Folder (FF), News Article (NA), Budget (Bgt), Invoice (Inv), Presentation (Prsnt), Questionnaire (Qnr), and Resume (Rsm).

Data-Driven Document Taxonomy Analysis. To verify Alg. 1, we collect the ID dataset from both RVL-CDIP and Laion-HR based on the 16 classes provided in RVL-CDIP. We sample OOD categories such as "Magazine" (M), "Comic" (C), "Guidebook" (G), "Yearbook" (Y), "Worksheet" (W), and "Open Book" (OB), *etc*, from $\mathcal{Y}$ and collect the OOD data from Laion-HR. In the Appendix, Table 7 shows OOD detection results for two variants: predicting 16 and 50 centroids separately. The K-means method with 50 centroids excels in detecting outliers across all categories. Fig. 7 (center) displays taxonomy expansion with HITL taxonomy cleaning. We start with an initial ID set with 10 classes selected from RVL-CDIP. At every step, we sample 10 detected outlier data. As the data increases, our outlier detection method successfully retrieves outliers for the majority of novel categories. Fig. 7 (left, right) illustrates the distribution of "Comic" and ID data, where "Comic" is detected as an outlier in the first step. Red color indicates the detected outlier samples.

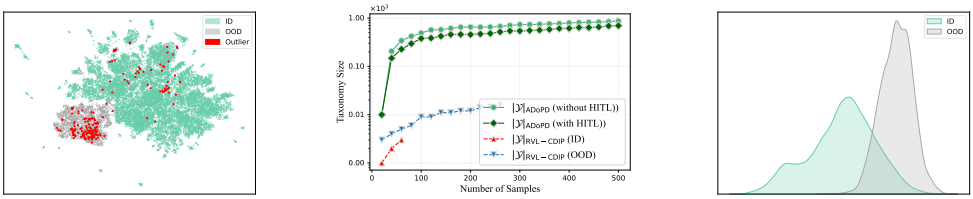

Figure 7: Visualization of outlier detection, taxonomy expansion, and OOD score distributions.

Responsible AI Analysis. During data cleaning, we conduct a comprehensive Responsible AI analysis, tackling biases in sensitive areas such as nudity, sexuality, and violence. We meticulously filter sensitive data with input from 15 diverse evaluators. Fig. 8 displays their geographic distribution. If any evaluator deems an image inappropriate, we label it as sensitive. After review, we remove 9.29% of potentially sensitive images, ensuring the majority of the 120K images remain non-sensitive. This rigorous process guarantees a safer and less biased dataset, promoting fairness and inclusivity in our models.

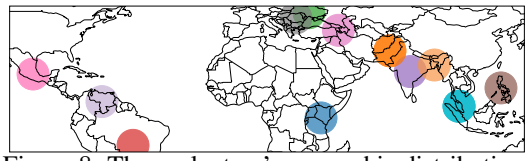

Figure 8: The evaluators' geographic distribution.

5 Conclusion

This paper introduces ADOPD, a dataset for document page decomposition and description, bridging gaps between document, natural image, vision-language, and NLP domains. It outlines data collection, taxonomy analysis, model-assisted annotation, and HITL processes. We comprehensively analyze ADOPD across four tasks, aiming to unlock opportunities for future exploration in document understanding and reasoning. The release of ADOPD aims to support foundational models for document understanding, catalyzing advancements in document analysis.

REFERENCES

Yejin Bang, Samuel Cahyawijaya, Nayeon Lee, Wenliang Dai, Dan Su, Bryan Wilie, Holy Lovenia, Ziwei Ji, Tiezheng Yu, Willy Chung, et al. A multitask, multilingual, multimodal evaluation of chatgpt on reasoning, hallucination, and interactivity. In *IJCNLP-AACL*, 2023.

Zhaowei Cai and Nuno Vasconcelos. Cascade r-cnn: High quality object detection and instance segmentation. *TPAMI*, 2019.

Mathilde Caron, Hugo Touvron, Ishan Misra, Hervé Jégou, Julien Mairal, Piotr Bojanowski, and Armand Joulin. Emerging properties in self-supervised vision transformers. In *ICCV*, 2021.

Kai Chen, Jiaqi Wang, Jiangmiao Pang, Yuhang Cao, Yu Xiong, Xiaoxiao Li, Shuyang Sun, Wansen Feng, Ziwei Liu, Jiarui Xu, Zheng Zhang, Dazhi Cheng, Chenchen Zhu, Tianheng Cheng, Qijie Zhao, Buyu Li, Xin Lu, Rui Zhu, Yue Wu, Jifeng Dai, Jingdong Wang, Jianping Shi, Wanli Ouyang, Chen Change Loy, and Dahua Lin. MMDetection: Open mmlab detection toolbox and benchmark. *arXiv preprint arXiv:1906.07155*, 2019.

Zhe Chen, Yuchen Duan, Wenhai Wang, Junjun He, Tong Lu, Jifeng Dai, and Yu Qiao. Vision transformer adapter for dense predictions. In *ICLR*, 2022.

Bowen Cheng, Alexander G. Schwing, and Alexander Kirillov. Per-pixel classification is not all you need for semantic segmentation. In *NeurIPS*, 2021.

Hiuyi Cheng, Peirong Zhang, Sihang Wu, Jiaxin Zhang, Qiyuan Zhu, Zecheng Xie, Jing Li, Kai Ding, and Lianwen Jin. M6doc: A large-scale multi-format, multi-type, multi-layout, multi-language, multi-annotation category dataset for modern document layout analysis. In *CVPR*, 2023.

CLIP ViT-G/14. Clip vit-g/14. `https://huggingface.co/laion/CLIP-ViT-g-14-laion2B-s12B-b42K`. 2023.

Michael Denkowski and Alon Lavie. Meteor universal: Language specific translation evaluation for any target language. In *WMT*, 2014.

Yuning Du, Chenxia Li, Ruoyu Guo, Cheng Cui, Weiwei Liu, Jun Zhou, Bin Lu, Yehua Yang, Qiwen Liu, Xiaoguang Hu, et al. Pp-ocrv2: Bag of tricks for ultra lightweight ocr system. *arXiv preprint arXiv:2109.03144*, 2021.

Mark Everingham, Luc Van Gool, Christopher KI Williams, John Winn, and Andrew Zisserman. The pascal visual object classes (voc) challenge. *IJCV*, 2010.

Luciano Floridi and Massimo Chiriatti. Gpt-3: Its nature, scope, limits, and consequences. *Minds and Machines*, 30:681–694, 2020.

Golnaz Ghiasi, Yin Cui, Aravind Srinivas, Rui Qian, Tsung-Yi Lin, Ekin D. Cubuk, Quoc V. Le, and Barret Zoph. Simple copy-paste is a strong data augmentation method for instance segmentation. In *CVPR*, 2021.

Jiuxiang Gu, Jason Kuen, Vlad I Morariu, Handong Zhao, Rajiv Jain, Nikolaos Barmpalios, Ani Nenkova, and Tong Sun. Unified pretraining framework for document understanding. In *NeurIPS*, 2021.

Jiuxiang Gu, Yifei Ming, Yi Zhou, Jason Kuen, Vlad I Morariu, Handong Zhao, Ruiyi Zhang, Nikolaos Barmpalios, Anqi Liu, Yixuan Li, et al. A critical analysis of out-of-distribution detection for document understanding. In *EMNLP*, 2023.

Adam W Harley, Alex Ufkes, and Konstantinos G Derpanis. Evaluation of deep convolutional nets for document image classification and retrieval. In *ICDAR*, 2015.

Yupan Huang, Tengchao Lv, Lei Cui, Yutong Lu, and Furu Wei. Layoutlmv3: Pre-training for document ai with unified text and image masking. In *ACMMM*, 2022.

Wenyu Jiang, Hao Cheng, Mingcai Chen, Chongjun Wang, and Hongxin Wei. Dos: Diverse outlier sampling for out-of-distribution detection. In *ICLR*, 2024.

Geewook Kim, Teakgyu Hong, Moonbin Yim, JeongYeon Nam, Jinyoung Park, Jinyeong Yim, Wonseok Hwang, Sangdoo Yun, Dongyoon Han, and Seunghyun Park. Ocr-free document understanding transformer. In *ECCV*, 2022.

Alexander Kirillov, Eric Mintun, Nikhila Ravi, Hanzi Mao, Chloe Rolland, Laura Gustafson, Tete Xiao, Spencer Whitehead, Alexander C. Berg, Wan-Yen Lo, Piotr Dollár, and Ross Girshick. Segment anything. *arXiv:2304.02643*, 2023.

Laion High Resolution. Laion. `https://huggingface.co/datasets/laion/laion-high-resolution`. 2023.

Jordy Landeghem, Rubén Tito, Łukasz Borchmann, Michał Pietruszka, Paweł Józiak, Rafał Powalski, Dawid Jurkiewicz, Mickaël Coustaty, Bertrand Ackaert, Ernest Valveny, et al. Document understanding dataset and evaluation (dude). In *ICCV*, 2023.

Joonho Lee, Hideaki Hayashi, Wataru Ohyama, and Seiichi Uchida. Page segmentation using a convolutional neural network with trainable co-occurrence features. In *ICDAR*, 2019.

David D. Lewis, Gady Agam, Shlomo Engelson Argamon, Ophir Frieder, David A. Grossman, and Jefferson Heard. Building a test collection for complex document information processing. *SIGIR*, 2006.

Junlong Li, Yiheng Xu, Tengchao Lv, Lei Cui, Cha Zhang, and Furu Wei. Dit: Self-supervised pre-training for document image transformer. In *ACMMM*, 2022a.

Junnan Li, Dongxu Li, Caiming Xiong, and Steven Hoi. Blip: Bootstrapping language-image pre-training for unified vision-language understanding and generation. In *ICML*, 2022b.

Junnan Li, Dongxu Li, Silvio Savarese, and Steven Hoi. Blip-2: Bootstrapping language-image pre-training with frozen image encoders and large language models. *arXiv preprint arXiv:2301.12597*, 2023.

Kai Li, Curtis Wigington, Chris Tensmeyer, Handong Zhao, Nikolaos Barmpalios, Vlad I Morariu, Varun Manjunatha, Tong Sun, and Yun Fu. Cross-domain document object detection: Benchmark suite and method. In *CVPR*, 2020a.

Minghao Li, Yiheng Xu, Lei Cui, Shaohan Huang, Furu Wei, Zhoujun Li, and Ming Zhou. Docbank: A benchmark dataset for document layout analysis. In *COLING*, 2020b.

Peizhao Li, Jiuxiang Gu, Jason Kuen, Vlad Morariu, Handong Zhao, Rajiv Jain, Varun Manjunatha, and Hongfu Liu. Selfdoc: Self-supervised document representation learning. In *CVPR*, 2021.

Chin-Yew Lin. Rouge: A package for automatic evaluation of summaries. In *Text summarization branches out*, pp. 74–81, 2004.

Tsung-Yi Lin, Michael Maire, Serge Belongie, James Hays, Pietro Perona, Deva Ramanan, Piotr Dollár, and C Lawrence Zitnick. Microsoft coco: Common objects in context. In *ECCV*, 2014.

Ze Liu, Yutong Lin, Yue Cao, Han Hu, Yixuan Wei, Zheng Zhang, Stephen Lin, and Baining Guo. Swin transformer: Hierarchical vision transformer using shifted windows. In *CVPR*, 2021.

Minesh Mathew, Dimosthenis Karatzas, and CV Jawahar. Docvqa: A dataset for vqa on document images. In *WACV*, 2021.

Puneet Mathur, Rajiv Jain, Jiuxiang Gu, Franck Dernoncourt, Dinesh Manocha, and Vlad Morariu. Docedit: Language-guided document editing. In *AAAI*, 2023.

Yifei Ming, Ziyang Cai, Jiuxiang Gu, Yiyou Sun, Wei Li, and Yixuan Li. Delving into out-of-distribution detection with vision-language representations. In *NeurIPS*, 2022.

Ajoy Mondal, Peter Lipps, and CV Jawahar. Iiit-ar-13k: a new dataset for graphical object detection in documents. In *DAS*, 2020.

Maxime Oquab, Timothée Darcet, Théo Moutakanni, Huy Vo, Marc Szafraniec, Vasil Khalidov, Pierre Fernandez, Daniel Haziza, Francisco Massa, Alaaeldin El-Nouby, et al. Dinov2: Learning robust visual features without supervision. *TMLR*, 2023.

Nazih Ouwayed and Abdel Belaïd. A general approach for multi-oriented text line extraction of handwritten documents. *IJDAR*, 2012.

Kishore Papineni, Salim Roukos, Todd Ward, and Wei-Jing Zhu. Bleu: a method for automatic evaluation of machine translation. In *ACL*, 2002.

Niki Parmar, Ashish Vaswani, Jakob Uszkoreit, Lukasz Kaiser, Noam Shazeer, Alexander Ku, and Dustin Tran. Image transformer. In *ICML*, 2018.

Birgit Pfitzmann, Christoph Auer, Michele Dolfi, Ahmed S Nassar, and Peter Staar. Doclaynet: A large human-annotated dataset for document-layout segmentation. In *SIGKDD*, 2022.

Devashish Prasad, Ayan Gadpal, Kshitij Kapadni, Manish Visave, and Kavita Sultanpure. Cascadetabnet: An approach for end to end table detection and structure recognition from image-based documents. In *CVPRW*, 2020.

Lu Qi, Jason Kuen, Tiancheng Shen, Jiuxiang Gu, Weidong Guo, Jiaya Jia, Zhe Lin, and Ming-Hsuan Yang. High-quality entity segmentation. In *ICCV*, 2023.

Alec Radford, Jeffrey Wu, Rewon Child, David Luan, Dario Amodei, Ilya Sutskever, et al. Language models are unsupervised multitask learners. *OpenAI blog*, 1(8):9, 2019.

Alec Radford, Jong Wook Kim, Chris Hallacy, Aditya Ramesh, Gabriel Goh, Sandhini Agarwal, Girish Sastry, Amanda Askell, Pamela Mishkin, Jack Clark, et al. Learning transferable visual models from natural language supervision. In *ICML*, 2021.

Yongming Rao, Wenliang Zhao, Yansong Tang, Jie Zhou, Ser-Lam Lim, and Jiwen Lu. Hornet: Efficient high-order spatial interactions with recursive gated convolutions. In *NeurIPS*, 2022.

Shaoqing Ren, Kaiming He, Ross Girshick, and Jian Sun. Faster r-cnn: Towards real-time object detection with region proposal networks. In *NeurIPS*, 2015.

RSM Saad, RI Elanwar, NSA Kader, S Mashali, and M Betke. Bce-arabic-v1 dataset: towards interpreting arabic document images for people with visual impairments categories and subject descriptors. *PETRA*, 2016.

Brandon Smock, Rohith Pesala, and Robin Abraham. Pubtables-1m: Towards comprehensive table extraction from unstructured documents. In *CVPR*, 2022.

Zineng Tang, Ziyi Yang, Guoxin Wang, Yuwei Fang, Yang Liu, Chenguang Zhu, Michael Zeng, Cha Zhang, and Mohit Bansal. Unifying vision, text, and layout for universal document processing. In *CVPR*, 2023.

Ramakrishna Vedantam, C Lawrence Zitnick, and Devi Parikh. Cider: Consensus-based image description evaluation. In *CVPR*, 2015.

Thomas Wolf, Lysandre Debut, Victor Sanh, Julien Chaumond, Clement Delangue, Anthony Moi, Pierric Cistac, Tim Rault, Rémi Louf, Morgan Funtowicz, Joe Davison, Sam Shleifer, Patrick von Platen, Clara Ma, Yacine Jernite, Julien Plu, Canwen Xu, Teven Le Scao, Sylvain Gugger, Mariama Drame, Quentin Lhoest, and Alexander M. Rush. Transformers: State-of-the-art natural language processing. In *EMNLP*, 2020.

Yuxin Wu, Alexander Kirillov, Francisco Massa, Wan-Yen Lo, and Ross Girshick. Detectron2. `https://github.com/facebookresearch/detectron2`, 2019.

Xu Zhong, Jianbin Tang, and Antonio Jimeno Yepes. Publaynet: largest dataset ever for document layout analysis. In *ICDAR*, 2019.

Xizhou Zhu, Weijie Su, Lewei Lu, Bin Li, Xiaogang Wang, and Jifeng Dai. Deformable detr: Deformable transformers for end-to-end object detection. In *ICLR*, 2021.

A APPENDIX

A.1 ABLATION STUDY OF OUTLIER DETECTION

Table 7 presents OOD detection results obtained using our K-means-based method, with two variants: predicting 16 and 50 centroids separately. The K-means method with 50 centroids excels in OOD detection across all categories, showcasing its effectiveness in identifying outlier data.

Table 7: Performance of outlier detection methods in dataset exploration.

ID	Outlier Score	AUROC (%)↑						FPR95 (%)↓					
		M	C	G	Y	W	OB	M	C	G	Y	W	OB
RVL-CDIP	K-Means (16)	99.99	99.99	99.99	99.99	99.85	99.98	0.01	0.11	0.00	0.00	0.67	0.08
	K-Means (50)	99.99	99.99	99.99	99.99	99.87	99.97	0.01	0.03	0.00	0.00	0.53	0.16
	MCM	80.23	94.50	91.36	92.44	91.92	89.57	80.58	31.27	51.01	42.11	44.06	49.37
ADOPD	K-Means (16)	86.28	90.86	89.08	87.64	59.16	78.13	33.02	21.40	28.05	39.61	82.66	65.74
	K-Means (50)	86.89	92.86	89.41	87.46	59.90	78.71	32.35	27.69	29.53	39.85	80.46	65.70
	MCM	71.42	91.13	86.69	87.58	87.58	84.16	89.89	45.18	68.23	54.39	56.66	60.76

A.1.1 ABLATION STUDY OF PROMPTS

Table 8 shows the results of human evaluation for various prompts. In each case, we randomly chose 100 images for comparison and instructed human evaluators to exclude any incorrect samples.

Table 8: Human evaluation of prompt-guided context-aware captioning.

Prompt			Prompt		
① You are an expert in generating descriptive captions for documents. Provide a concise reference description of the document: `<image caption>` and some image attributes: `<tags>` . The document has words extracted from the image: `<ocr words>` . Create a comprehensive and precise caption to describe the document content.	27		② You are an expert in generating descriptive captions for documents. Provide a concise reference description of the document: `<image caption>` and some image attributes: `<tags>` . The document has words extracted from the image: `<ocr words>` . Create a comprehensive and precise caption to describe the document content.	38	
③ You are an expert in generating caption for document image. The document includes some visual attributes: `<tags>` , and contains text content: `<ocr words>` . There is a possible coarse caption for the document: `<image caption>` . Now, in your own words, please describe the document's content, referencing the provided information.	41	61	④ You are an expert in generating descriptive captions for documents. Provide a concise reference description of the document: `<image caption>` and some attributes: `<tags>` . The document has some text content: `<ocr words>` . Please describe the document's content, referencing the provided information. Create a comprehensive and precise caption to describe the document content.	47	48
⑤ You are an expert in generating caption for document image. The document includes some visual attributes: `<tags>` , and contains text content: `<ocr-summary>` . There is a possible coarse caption for the document: `<image caption>` . Now, in your own words, please describe the document's content, referencing the provided information.		44	⑥ You are an expert in generating descriptive captions for documents. Provide a concise reference description of the document: `<image caption>` and some attributes: `<tags>` . The document has some text content: `<ocr-summary>` . Please describe the document's content, referencing the provided information. Create a comprehensive and precise caption to describe the document content.		49

As outlined in Sec.3.2, we utilize four prompts to generate annotated document labels, leveraging linguistic, visual, layout, and multi-modal information. Detailed prompts are listed in Table9. Although the format of prompts focused on different aspects is consistent, different prompts include varying input items (indicated by check signals in Table9). The red texts in the table represent inputs or variables related to prompt selection (as shown in Table10).

Considering the order of input items may impact the quality of taxonomy generation, we conducted experiments on different prompts to investigate the optimal input order. Given that some sentences are fixed for all prompts, our study focuses on the influence of the order of the prompt sentences containing inputs (Row 3-7 in Table 9). To simplify the study, we specifically consider Rows 6 and 7, which both represent high-level information for the entire document images and should be put together, while the order between them remains undecided. In the study, human annotators assess the output labels of the prompts and vote on them. They consider the relevance between the document image and labels and eliminate orders that result in conflicting or ambiguous labels. We then count the number of votes for each order to determine the most favored order.

1. **Order of Visual and Textual Prompt Inputs**
   - **i. Visual** We shuffle the order of input items of visual prompt (3, 6, and 7) into 4 different orders while keeping 6 and 7 adjacent: 3-6-7, 3-7-6, 6-7-3, and 7-6-3. The investigation result is shown Fig. 9(a)
   - **ii. Textual** Similar to visual prompt, 4 orders are investigated: 5-6-7, 5-7-6, 6-7-5, and 7-6-5. The investigation result is shown Fig. 9(b)

   Considering the results of the Visual and Textual Prompt, we choose 3-6-7 and 5-6-7 as the input order of our prompt. We can also find that it would be better to input the description (Row 6) before the pre-labels (Row 7) and put it at the end of the list. We will keep this order in the following study.
2. **Order of Layout Prompt Inputs** We investigated two different layout orders: 4-5-6-7 and 5-4-6-7. Considering that text space may influence layout comprehension, we classified a document with a text area larger than 0.2 of the size as text-rich. In our study, we present the results separately

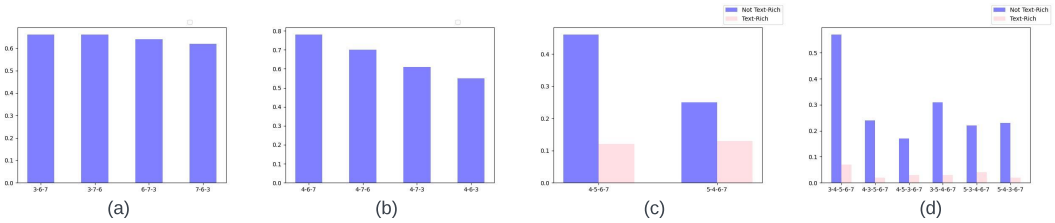

Figure 9: Human evaluation result for different order of Visual and Textual prompt inputs.

based on this criterion in Fig. 9(c). The figure illustrates that when the text is rich, the order 5-4-6-7 receives more votes, while 4-5-6-7 is favored otherwise. Consequently, we choose to use the order 5-4-6-7 when the text is rich and 4-5-6-7 when the text is not as text-rich.

3. **Order of Mutimodal Prompt Inputs** Multimodal prompts predict the labels using all provided information. Building on previous findings, we standardized the order of Rows 6 and 7, placing them at the bottom of the inputs. For the remaining 3 inputs, we shuffled them to create a total of 6 different orders: 3-4-5-6-7, 4-3-5-6-7, 4-5-3-6-7, 3-5-4-6-7, 5-3-4-6-7, and 5-4-3-6-7. As shown in Fig. 9, the results suggest that the order 3-4-5-6-7 yields the best performance among all orders. After obtaining labels with different information, we summarize them into 10 categories to classify the document. The detailed prompt is shown in Table 11.

Table 9: Prompts from four aspects (textual, visual, layout, and multimodal).

		Dataset	Visual	Textual	Layout	Multimodal
	1	You are an expert in seeing and understanding a given document image.	✓	✓	✓	✓
	2	Here is the relevant information about the document:	✓	✓	✓	✓
	3	Visual elements may appear in the document: visual tag0, [visual tag1, visual tag2, ...]	✓	✗	✗	✓
	4	OCR layout information: [[OCR1, bbox1], [OCR2, bbox2] ...]; In each layout item, the first 4 numbers (x1, y1, x2, y2) are normalized coordinates, and the last string is the detected OCR text	✗	✗	✓	✓
	5	The textual content in the document are: [OCR1, OCR2, ...]	✗	✓	✓	✓
	6	A possible coarse description of this document: Caption	✓	✓	✓	✓
	7	Possible overall categories of this document, such as: [Pre-label1, Pre-label2, ...]	✓	✓	✓	✓
	8	You will primarily focus on USED RESOURCE to provide 5 labels related to the conception of "CONCEPT" of documents in your own word. The labels should be significantly representative of this document within 5 words.	✓	✓	✓	✓
	9	Here is an example for output: [1. {Lable1}, 2. {Lable1}, ...] . The labels should not contain any specific content shown in the document.	✓	✓	✓	✓

Table 10: Variable settings for prompts.

Modality	USED RESOURCE
Visual	The possible visual elements while considering other mentioned details such as description, and possible categories 1
Textual	The textual content summarization while considering other mentioned details such as description, and possible categories
Layout	The layout information and design of the document while considering relevant details such as description, visual elements, textual content, and possible categories
Multimodal	All the information above such as description, visual elements, textual content, and possible categories and layout information

Table 11: Prompts for label summary.

		Prompt Sentence
	1	You are a languistic expert that can well understand the difference between phrases.
	2	You will receive 4 lists of labels of the same document image from 4 annotators. They focus on visual, linguistic, layout, and multimodal aspects of the image.
	3	You should come out 10 most common conceptions from the list with in 4 words for each.
	4	The labels given by the visual-focused annotator are: VisualLabel1, VisualLabel2, VisualLabel3 ...
	5	The labels given by the linguistic-focused annotator are: TextLabel1, TextLabel2, TextLabel3 ...
	6	The labels given by the layout-focused annotator are: LayoutLabel1, LayoutLabel2, LayoutLabel3 ...
	7	The labels given by the multimdal-focused annotator are: MultimdalLabel1, MultimdalLabel2, MultimdalLabel3 ...
	8	Here is a example for output: [1. {Lable1}, 2. {Lable1}, ...].

A.2 Data Annotation Process Analysis

A.2.1 Image Analysis

Fig. 11 illustrates our analysis of the image data, showcasing the high resolution of our dataset. During the annotation process, despite some images having high resolution, the text appears blurry. We require annotators to skip labeling such images to ensure clear visibility of text in all pictures. During training, we resize each image to 1024 x 1024, but during testing, we use the raw resolution.

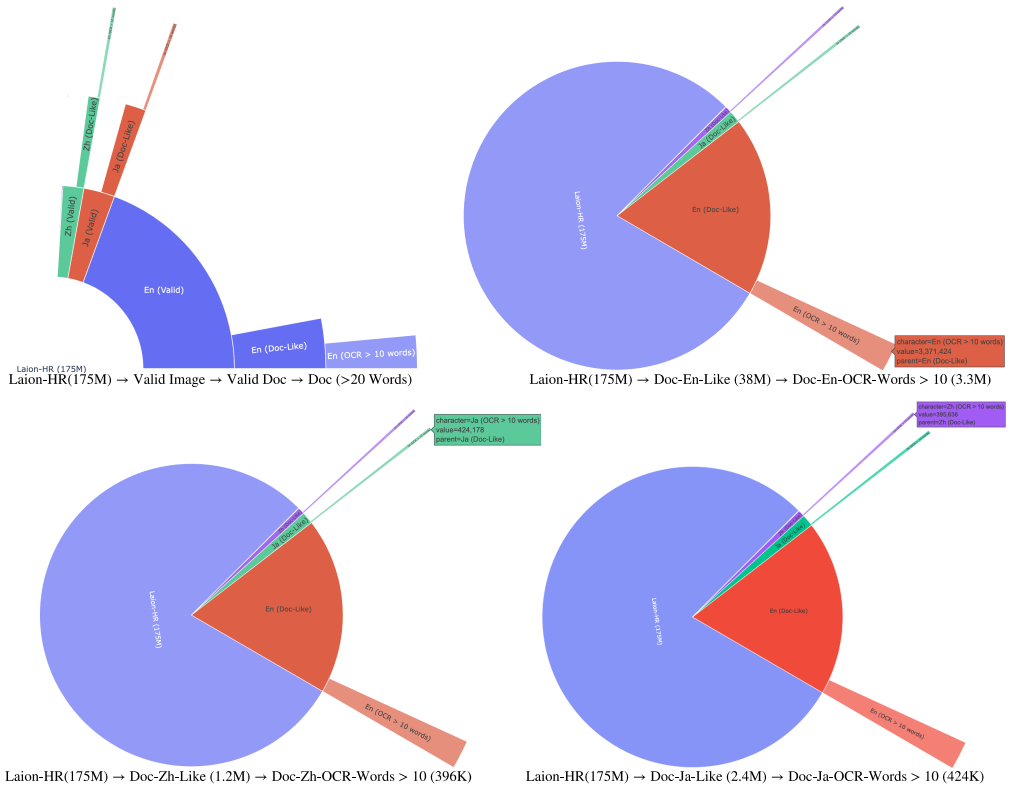

Figure 10: Data Selection Proportion Diagram.

A.2.2 Model-Enhanced Annotation Cost Analysis

In Fig. **??**, we analyze the variation in Doc2Mask annotation costs with the improvement of the model. As the cost of annotating data depends on various factors such as the complexity, type, language, and other aspects of the current batch of images. The displayed cost changes represent a subset of the ADOPD (English) dataset. It is evident that with model enhancement, there is a downward trend in relative costs. Here, the relative cost is calculated based on the cost of modifying and adding masks for each image, with the y-axis representing normalized costs rather than the actual cost for each image. In practice, costs are associated with masks and boxes, so the varying number of masks or boxes per image can lead to different costs.

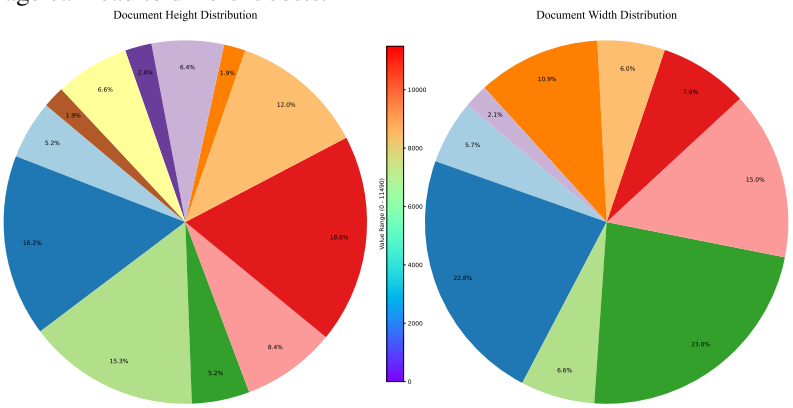

Figure 11: Distribution of the document image sizes for ADOPD.

Figure 12: ADOPD (En) Model-Assisted Annotation Comparison(Left) EntitySeg pre-label and human annotations. (Right) Doc2Mask (finetune on ADOPD) pre-label and manual annotations.

Figure 13: ADOPD (Non-En) Model-Assisted Annotation Comparison(Left) Doc2Mask (finetune on ADOPD-En) pre-label (Zh) and human annotations. (Right) Doc2Mask (finetune on ADOPD-En) pre-label (Ja) and manual annotations.

A.2.3 Model-Assisted Annotation Data Visualization

A.3 Multi-Lingual Doc2Box Samples

Figure 14: Doc2Box Samples.